Proceedings of HT2005
2005 ASME Summer Heat Transfer Conference
July 17-22, 2005, San Francisco, California, USA

HT2005-72078

A NON-BOILING TWO-PHASE FLOW HEAT TRANSFER CORRELATION FOR DIFFERENT FLOW PATTERNS AND PIPE INCLINATION ANGLES

Afshin J. Ghajar and Jae-yong Kim
School of Mechanical and Aerospace Engineering
Oklahoma State University,
Stillwater, OK 74078, USA
E-mail: ghajar@ceat.okstate.edu

ABSTRACT

Local heat transfer coefficients and flow parameters were measured for air-water flow in a pipe in the horizontal and slightly upward inclined positions (2°, 5°, and 7°) and different flow patterns. The test section was a 27.9 mm stainless steel pipe with a length to diameter ratio of 100. A total of 408 data points were taken on horizontal and inclined positions by carefully coordinating the liquid and gas superficial Reynolds number combinations. These superficial Reynolds numbers were duplicated for each inclination angle. The heat transfer data were measured under a uniform wall heat flux boundary condition ranging from about 3000 W/m^2 to 10,600 W/m^2. The superficial Reynolds numbers ranged from about 820 to 26,000 for water and from about 560 to 48,000 for air. These experimental data including different flow patterns and inclination angles were successfully correlated by a general two-phase heat transfer correlation with an overall mean deviation of –4.22%, a standard deviation of 12.5%, and a deviation range of –30.7 to 37.0%. Ninety percent (90%) of the data were predicted within ± 20% deviation.

INTRODUCTION

Gas-liquid two-phase flow in pipes is commonly observed in many industrial applications, such as oil wells and pipelines, solar collectors, chemical reactors, and nuclear reactors, and its hydrodynamic and thermal conditions are dependent upon the interaction between the two phases. However, due to the complex nature of the two-phase gas-liquid flow, the accessible heat transfer data and applicable correlations for non-boiling two-phase flow in horizontal and inclined pipes covering various flow patterns and inclined positions are limited in the literature. Most of the available heat transfer correlations are often limited by specific flow pattern or flow orientation. A comprehensive discussion of the available experimental data and heat transfer correlations for forced convective heat transfer during gas-liquid two-phase flow in vertical and horizontal pipes, including flow patterns and fluid combinations is provided by Kim et al. (1999). However, due to the complex nature of the two-phase gas-liquid flow, no systematic investigation has been conducted to document the influence of flow pattern and inclination angle on the two-phase heat transfer. The only available information on the effect of inclination in the literature is from Hetsroni et al. (1998), and their study was qualitative in nature and limited to slug flow. Their experimental work measured the local heat transfer, using infrared thermography, as a function of slug frequency, slug length and height, inclination angle, and Froude number. Inclination angles were limited to 2° and 5°. They concluded that there was a drastic increase in heat transfer with only slight increases in inclination angle. The authors provided no quantitative information to support the observed increase in the heat transfer. Later, Trimble et al. (2002) quantitatively investigated the effect of inclination on heat transfer in slug flow. In their experimental study, the 2° and 5° data showed an average increase over the horizontal position of about 10% and 20%, respectively. However, their investigation was limited to only one flow pattern (slug flow) and was exploratory in nature and was not conducted systematically.

The objectives of this study were to extend the knowledge base by gathering quality non-boiling, two-phase, two-component heat transfer data in the horizontal and inclined positions with various flow patterns, and analyze their behavior and extend the capability of a general overall heat transfer coefficient correlation which was developed by our research team, see Kim et al. (2000). In order to achieve this goal, the nature of the heat transfer in air-water two-phase flow was investigated by comparing the two-phase heat transfer data that were obtained by systematically varying the air or water flow rates (flow pattern) and the pipe inclination angle.

NOMENCLATURE

C constant value of the leading coefficient in Eqs. (1) and (6), dimensionless
D inside diameter of a circular tube, m
F_P flow pattern factor, Eq. (3), dimensionless
F_S shape factor, Eq. (4), dimensionless
g acceleration due to gravity, m/s^2
h heat transfer coefficient, W/m^2·K
h_G heat transfer coefficient as if gas alone were flowing, W/m^2·K
h_L heat transfer coefficient as if liquid alone were flowing, W/m^2·K
h_{TP} overall mean two-phase heat transfer coefficient, Eq. (1), W/m^2·K
I inclination factor, Eq. (5), dimensionless
K slip ratio, dimensionless
L length of heat transfer test section, m
m constant exponent value on the quality ratio term in Eqs. (1) and (6), dimensionless
$\dot{m}$ mass flow rate, kg/s or kg/min
N_{st} number of thermocouple stations
n constant exponent value on the void fraction ratio term in Eqs. (1) and (6), dimensionless
Pr Prandtl number, dimensionless
p constant exponent value on the Prandtl number ratio term in Eqs. (1) and (6), dimensionless
q constant exponent value on the viscosity ratio term in Eqs. (1) and (6), dimensionless
Re Reynolds number, dimensionless
Re_L liquid in-situ Reynolds number, Eq. (7), dimensionless
r constant exponent value on the inclination factor in Eq. (6), dimensionless
S_L wetted-perimeter, m
u axial velocity, m/s
X Martinelli parameter $\left[=\left(\frac{1-x}{x}\right)^{0.9}\left(\frac{\rho_G}{\rho_L}\right)^{0.5}\left(\frac{\mu_L}{\mu_G}\right)^{0.1}\right]$, dimensionless
x quality or dryness fraction, dimensionless
Δz length of element in the finite-difference grid, m

Greek Symbols

α void fraction, dimensionless
μ dynamic viscosity, Pa-s
ρ density, kg/m^3
θ inclination angle of a pipe to the horizontal, rad

Superscript

$\bar{}$ local mean
$\sim$ non-dimensionalized

Subscripts

CAL calculated
EXP experimental
eq equilibrium state
eff effective
G gas phase
k index of thermocouple station in test section
L liquid phase
m mixture
SG superficial gas
SL superficial liquid
TP two-phase

Abbreviations

A annular flow
ABS slug/bubbly/annular transitional flow
AW wavy/annular transitional flow
BS slug/bubbly transitional flow
P plug flow
PS plug/slug transitional flow
S slug flow
SW slug/wavy transitional flow

DEVELOPMENT OF HEAT TRANSFER CORRELATION

In order to predict the heat transfer coefficient in two-phase flow, regardless of flow pattern and inclination angle, a new correlation is developed based on the work of Kim et al. (2000). In their work they assumed that the total gas-liquid two-phase heat transfer is the sum of the individual single-phase heat transfers of the gas and liquid, weighted by the volume of each phase present as shown in Eq. (1).

$$h_{TP} = (1-\alpha)\,h_L + \alpha\,h_G = (1-\alpha)\,h_L\left[1+\mathrm{C}\left\{\left(\frac{x}{1-x}\right)^m\left(\frac{\alpha}{1-\alpha}\right)^n\left(\frac{Pr_G}{Pr_L}\right)^p\left(\frac{\mu_G}{\mu_L}\right)^q\right\}\right] \quad (1)$$

Kim et al. (2000) correlation, Eq. (1), has been successfully applied to the experimental data taken in our laboratory [Kim and Ghajar (2002), Ghajar (2004), and Ghajar et al. (2004 a, b, c)]. However, the weighting factor (void fraction) used in our correlation does not fully account for the effect of different flow patterns and inclination angles on the two-phase heat transfer data. In the past we had to use different set of constants for different flow patterns (Kim and Ghajar, 2002) and inclination angles (Ghajar et al., 2004 a, c). Therefore, in order to handle the effect of various flow patterns and inclination angles on the two-phase heat transfer data with only one correlation, the flow pattern factor (F_P) and the inclination factor (I) were developed as shown below.

Flow Pattern Factor (Effective Wetted-Perimeter Relation)

The void fraction,α, which is the volume fraction of the gas-phase in the tube cross-sectional area, does not reflect the

actual wetted-perimeter, S_L, in the tube with respect to the corresponding flow pattern. For instance, the void fraction and the non-dimensionalized wetted-perimeter of a plug flow both approach unity, but in the case of an annular flow the void fraction is near zero and the wetted-perimeter is near unity. However, the estimation of the actual wetted-perimeter is very difficult due to the continuous interaction of the two phases in the tube. Therefore, instead of estimating the actual wetted-perimeter, modeling the effective wetted-perimeter is a more practical approach. In our model we have ignored the influence of the surface tension and the contact angle of each phase on the effective wetted-perimeter.

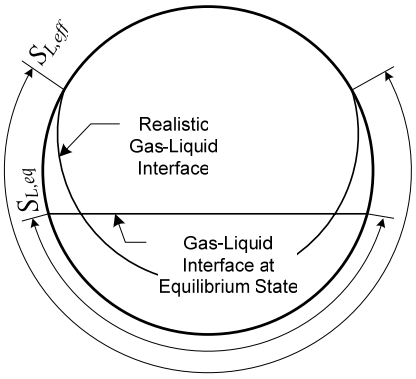

Figure 1. Gas-liquid interfaces and wetted-perimeters.

The wetted-perimeter at the equilibrium state, which can be calculated from the void fraction as shown in Eq. (2) is

$$\widetilde{S}_{L,eq}^2 = \left(\frac{S_{L,eq}}{\pi D}\right)^2 = 1-\alpha \qquad (2)$$

However, as shown in Fig. 1, the shape of the gas-liquid interface at the equilibrium state based on the void fraction, α, is far different from the one for the realistic case. As mentioned before, it can also be noticed from Eqs. (1) and (2) that the two-phase heat transfer correlation weighted by the void fraction is not capable of distinguishing the differences between the different flow patterns. Therefore, in order to capture the realistic shape of the gas-liquid interface, the flow pattern factor (F_P), an effective wetted-perimeter relation, which is a modified version of the equilibrium wetted-perimeter, Eq. (2), is proposed.

$$F_P = \widetilde{S}_{L,eff}^2 = \left(\frac{S_{L,eff}}{\pi D}\right)^2 = (1-\alpha) + \alpha F_S^2 \qquad (3)$$

where in the above equation for simplicity the effective wetted-perimeter relation ($\widetilde{S}_{L,eff}^2$) is refereed to as the flow pattern factor (F_P). The term F_S appearing in Eq. (3) above is referred to as shape factor which in essence is a modified and normalized Froude number. The shape factor (F_S) is defined as:

$$F_S = \frac{2}{\pi}\tan^{-1}\left(\sqrt{\frac{\rho_G (u_G - u_L)^2}{g\,D(\rho_L - \rho_G)\cos(\theta)}}\right) \qquad (4)$$

The shape factor, F_S, is applicable for slip ratios $K(=u_G/u_L) \geq 1$, which is common in gas-liquid flow, and represents the shape changes of the gas-liquid interface by the force acting on the interface due to the relative momentum and gravity forces.

Inclination Factor

Due to the density difference between gas and liquid, the liquid phase is much more affected by the orientation of flow (inclination). The detailed discussion of the inclination effect on the two-phase heat transfer is available in Ghajar et al. (2004b) and later in this paper. In order to account for the effect of inclination, the inclination factor, *I,* is proposed, which is defined as:

$$I = 1 + \frac{g\,D(\rho_L - \rho_G)\sin(\theta)}{\rho_L\, u_{SL}^2} \qquad (5)$$

where the term $[g\,D(\rho_L - \rho_G)\sin(\theta)]/[\rho_L\, u_{SL}^2]$ represents the relative force acting on the liquid phase in the flow direction due to the momentum and the gravity forces.

Heat Transfer Correlation

Now, introduce the two proposed factors for the flow pattern (F_P) and inclination (I) effects into our heat transfer correlation, Eq. (1). Substituting F_P for $(1-\alpha)$ which is the leading coefficient of h_L and introducing I as an additional power-law term in Eq. (1), the correlation becomes

$$h_{TP} = F_P\, h_L \left\{1 + C\left[\left(\frac{x}{1-x}\right)^m \left(\frac{1-F_P}{F_P}\right)^n \left(\frac{Pr_G}{Pr_L}\right)^p \left(\frac{\mu_G}{\mu_L}\right)^q (I)^r\right]\right\} \qquad (6)$$

where h_L comes from the Sieder and Tate (1936) correlation for turbulent flow. For the Reynolds number needed in the h_L calculation, the following relationship is used to evaluate the in-situ Reynolds number (liquid phase) rather than the superficial Reynolds number (Re_{SL}) as commonly used in the correlations available in the literature [see Kim et al. (1999)]:

$$Re_L = \left(\frac{\rho u D}{\mu}\right)_L = \frac{4\dot{m}_L}{\pi\sqrt{1-\alpha}\,\mu_L D} \qquad (7)$$

The values of the void fraction, α, used in Eqs. (3) and (7) are calculated based on the correlation provided by Chisholm (1973) in this study, which can be expressed as:

$$\alpha = \left[1 + \left(\frac{\rho_L}{\rho_m}\right)^{1/2}\left(\frac{1-x}{x}\right)\left(\frac{\rho_G}{\rho_L}\right)\right]^{-1} \qquad (8)$$

where $1/\rho_m = (1-x)/\rho_L + x/\rho_G$.

Note that any other well-known correlations for single-phase turbulent heat transfer and void fraction could have been used in place of the Sieder and Tate (1936) correlation and Chisholm (1973) correlation, respectively. The difference resulting from the use of different correlations will be absorbed during the determination of the values of the leading coefficient and exponents on the different parameters in Eq. (6).

EXPERIMENTAL SETUP AND DATA REDUCTION

A schematic diagram of the overall experimental setup for heat transfer and pressure drop measurements and flow visualizations in two-phase air-water pipe flow in horizontal and inclined positions is shown in Fig. 2. The test section is a 27.9 mm straight standard stainless steel schedule 10S pipe with a length to diameter ratio of a 100. The setup rests atop an aluminum I-beam that is supported by a pivoting foot and a stationary foot that incorporates a small electric screw jack. The I-beam is approximately 9 m in length and can be inclined to an angle of approximately 8° above horizontal.

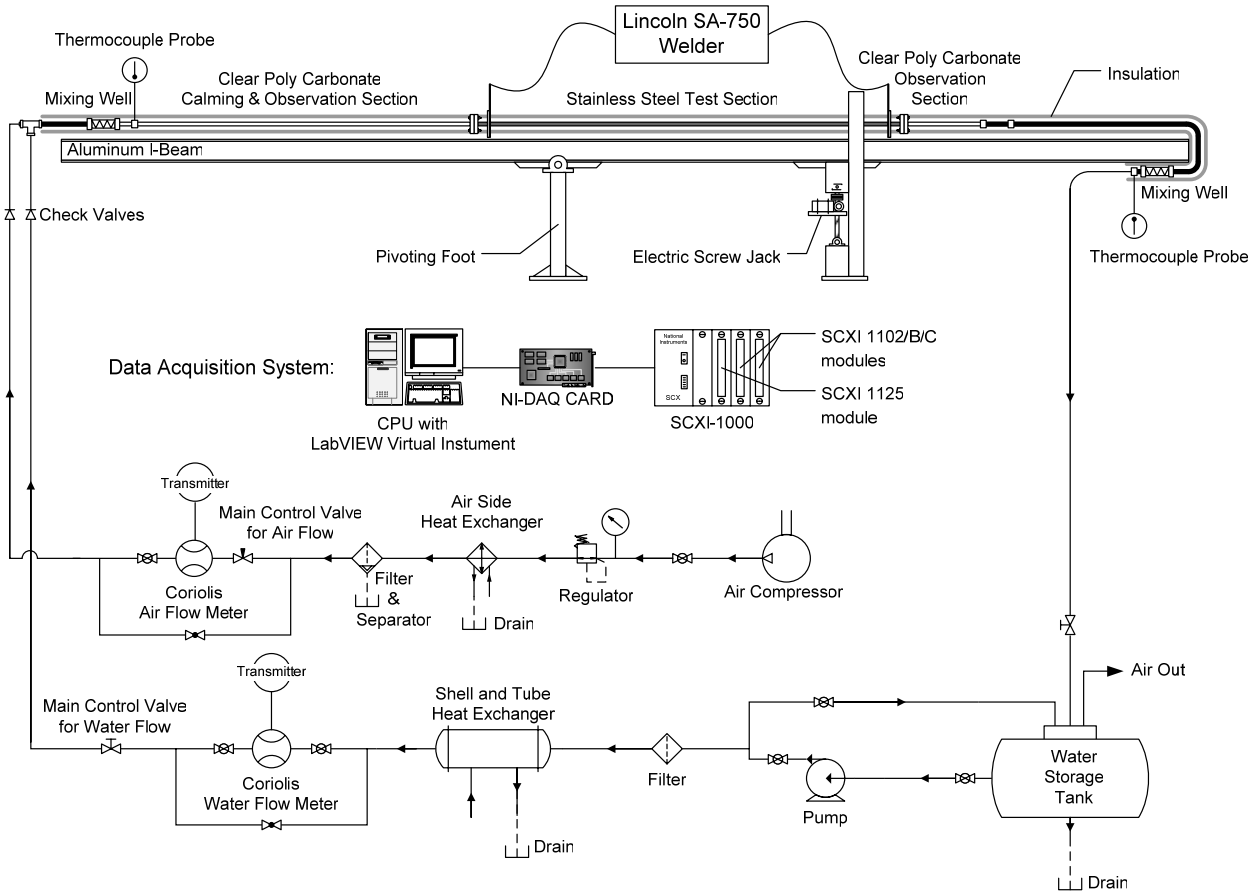

Figure 2. Schematic of experimental setup.

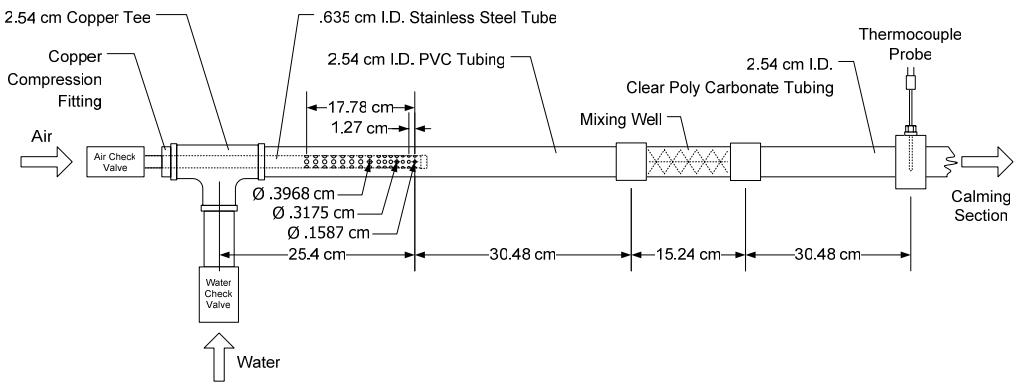

Figure 3. Air-water mixer

In order to apply uniform wall heat flux boundary conditions to the test section, copper plates were silver soldered to the inlet and exit of the test section. The uniform wall heat flux boundary condition was maintained by a Lincoln SA-750 welder. The entire length of the test section was wrapped using fiberglass pipe wrap insulation, followed by a thin polymer vapor seal to prevent moisture penetration.

In order to develop various two-phase flow patterns (by controlling the flow rates of gas and liquid), a two-phase gas and liquid flow mixer was used. The mixer consisted of a perforated stainless steel tube (6.35 mm I.D.) inserted into the liquid stream by means of a tee and a compression fitting. The end of the copper tube was silver-soldered. Four holes (3 rows of 1.59 mm, 4 rows of 3.18 mm, and 8 rows of 3.97 mm) were positioned at 90° intervals around the perimeter of the tube and this pattern was repeated at fifteen equally spaced axial locations along the length of the stainless steel tube (refer to Fig. 3). The two-phase flow leaving the mixer entered the transparent calming section. The calming section [clear polycarbonate pipe with 25.4 mm I.D. and L/D = 88] served as a flow developing and turbulence reduction device, and flow pattern observation section.

T-type thermocouple wires were cemented with Omegabond 101, an epoxy adhesive with high thermal conductivity and electrical resistivity, to the outside wall of the stainless steel test section (refer to Fig. 4). Omega EXPP-T-20-TWSH extension wires were used for relay to the data acquisition system. Thermocouples were placed on the outer surface of the tube wall at uniform intervals of 254 mm from the entrance to the exit of the test section. There were 10 thermocouple stations in the test section. All stations had four thermocouples, and they were labeled looking at the tail of the fluid flow with peripheral location "A" being at the top of the tube, "B" being 90° in the clockwise direction, "C" at the bottom of the tube, and "D" being 90° from the bottom in the clockwise sense (refer to Fig. 4). The inlet liquid and gas temperatures and the exit bulk temperature were measured by Omega TMQSS-125U-6 thermocouple probes. The thermocouple probe for the exit bulk temperature was placed after the mixing well. To ensure a uniform fluid bulk temperature at the inlet and exit of the test section, a mixing well was utilized. An alternating polypropylene baffle type static mixer for both gas and liquid phases was used. This mixer provided an overlapping baffled passage forcing the fluid to encounter flow reversal and swirling regions. The mixing well at the exit of the test section was placed below the clear polycarbonate observation section (after the test section), and before the liquid storage tank (refer to Fig. 1).

The fluids used in the test loop are air and water. The water is distilled and stored in a 55-gallon cylindrical polyethylene tank. A Bell & Gosset series 1535 coupled centrifugal pump was used to pump the water through a water filter. An ITT Standard model BCF 4063 one shell and two-tube pass heat exchanger removes the pump heat and the heat added during the test to maintain a constant inlet water temperature. From the heat exchanger, the water passes through a Micro Motion Coriolis flow meter (model CMF125) connected to a digital Field-Mount Transmitter (model RFT9739) that conditions the flow information for the data acquisition system. Once the water passes through the Coriolis flow meter it then passes through a 25.4 mm, twelve-turn gate valve that regulates the amount of flow that entered the test section. From this point, the water travels through a 25.4 mm flexible hose, through a one-way check valve, and into the test section. Air is supplied via an Ingersoll-Rand T30 (model 2545) industrial air compressor mounted outside the laboratory and isolated to reduce vibration onto the laboratory floor. The air passes through a copper coil submerged in a vessel of water to lower the temperature of the air to room temperature. The air is then filtered and condensate removed in a coalescing filter. The air flow is measured by a Micro Motion Coriolis flow meter (model CMF100) connected to a digital Field-Mount Transmitter (model RFT9739) and regulated by a needle valve. Air is delivered to the test section by flexible tubing. The water and air mixture is returned to the reservoir where it is separated and the water recycled.

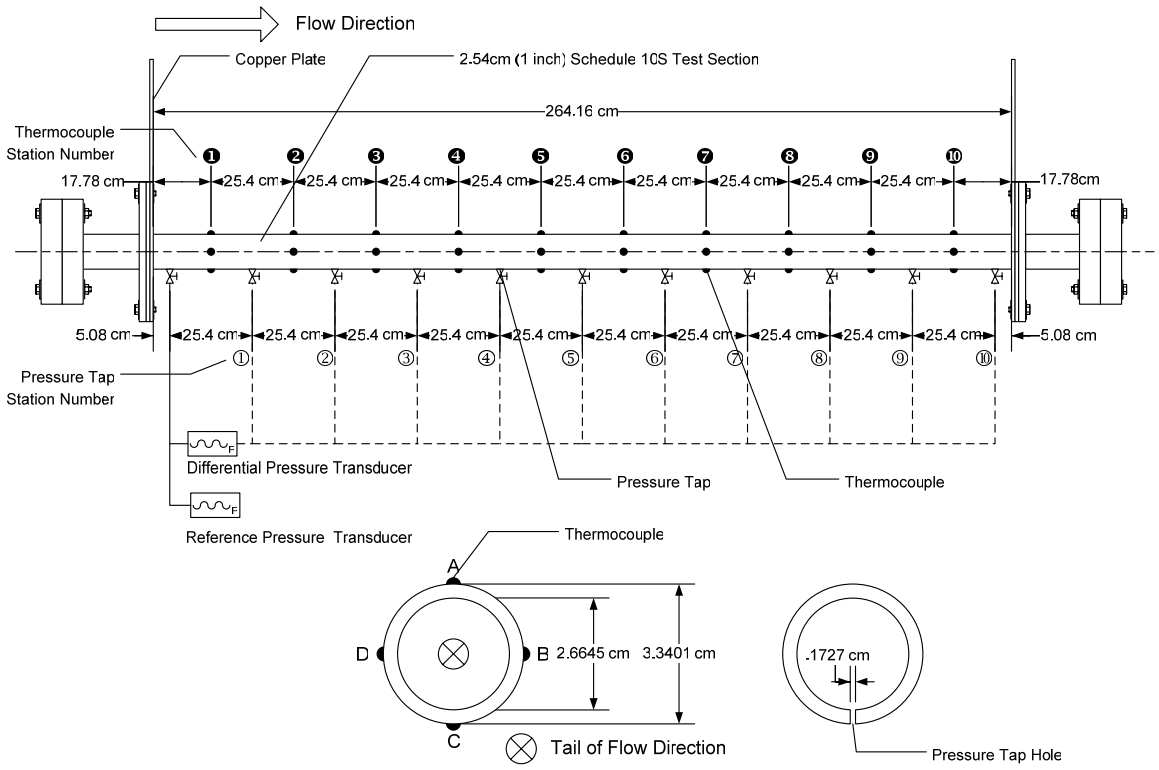

Figure 4. Test section.

The heat transfer measurements at uniform wall heat flux boundary condition were carried out by measuring the local outside wall temperatures at 10 stations along the axis of the tube and the inlet and outlet bulk temperatures in addition to other measurements such as the flow rates of gas and liquid, room temperature, voltage drop across the test section, and current carried by the test section. The peripheral heat transfer coefficient (local average) were calculated based on the knowledge of the pipe inside wall surface temperature and inside wall heat flux obtained from a data reduction program developed exclusively for this type of experiments (Ghajar and Zurigat, 1991). The local average peripheral values for inside wall temperature, inside wall heat flux, and heat transfer coefficient were then obtained by averaging all the appropriate individual local peripheral values at each axial location. The large variation in the circumferential wall temperature distribution, which is typical for two-phase gas-liquid flow in horizontal and slightly inclined tubes, leads to different heat transfer coefficients depending on which circumferential wall temperature was selected for the calculations. In two-phase heat transfer experiments, in order to overcome the unbalanced circumferential heat transfer coefficients, Eq. (9) was used to calculate an overall mean two-phase heat transfer coefficient (h_{TP}) for each test run.

$$h_{TP} = \frac{1}{L}\int \bar{h}\, dz = \frac{1}{L}\sum_{k=1}^{N_{ST}} \bar{h}_k\, \Delta z_k \qquad (9)$$

The data reduction program used a finite-difference formulation to determine the inside wall temperature and the inside wall heat flux from measurements of the outside wall temperature, the heat generation within the pipe wall, and the thermophysical properties of the pipe material (electrical resistivity and thermal conductivity). In these calculations, axial conduction was assumed negligible, but peripheral and radial conduction of heat in the tube wall were included. In addition, the bulk fluid temperature was assumed to increase linearly from the inlet to outlet.

A National Instruments data acquisition system was used to record and store the data measured during these experiments. The acquisition system is housed in an AC powered four-slot SCXI 1000 Chassis that serves as a low noise environment for signal conditioning. Three NI SCXI control modules are housed inside the chassis. There are two SCXI 1102/B/C modules and one SCXI 1125 module. From these three modules, input signals for all 40 thermocouples, the two thermocouple probes, voltmeter, and flow meters are gathered and recorded. The computer interface used to record the data is a LabVIEW Virtual Instrument (VI) program written for this specific application.

The uncertainty analyses of the overall experimental procedures using the method of Kline and McClintock (1953) showed that there is a maximum of 11.5% uncertainty for heat transfer coefficient calculations. Experiments under the same conditions were conducted periodically to ensure the repeatability of the results. The maximum difference between the duplicated experimental runs was within ±10%. More details of experimental setup and data reduction procedures can be found from Durant (2003).

The heat transfer data obtained with the present experimental setup were measured under a uniform wall heat flux boundary condition that ranged from 2730 to 10,690 W/m^2 and the resulting overall mean two-phase heat transfer coefficients (h_{TP}) ranged from 513 to 4419 W/m^2·K for horizontal flow. For these experiments, the liquid superficial Reynolds number (Re_{SL}) ranged from 821 to 26,043 (water mass flow rates from about 1.18 to 42.5 kg/min) and the gas superficial Reynolds numbers (Re_{SG}) ranged from 560 to 47,718 (gas mass flow rates from about 0.013 to 1.13 kg/min).

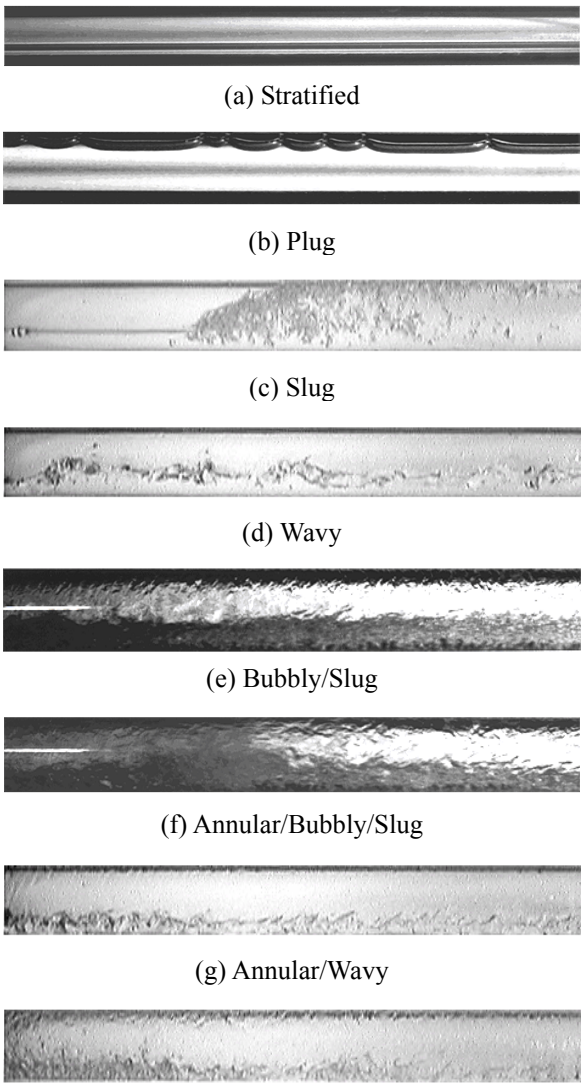

(a) Stratified

(b) Plug

(c) Slug

(d) Wavy

(e) Bubbly/Slug

(f) Annular/Bubbly/Slug

(g) Annular/Wavy

(h) Annular

Figure 5. Photographs of representative flow patterns (horizontal flow and isothermal).

RESULTS AND DISCUSSION

Flow Patterns

Due to the multitude of flow patterns and the various interpretations accorded to them by different investigators, no uniform procedure exists at present for describing and classifying them. In our reported studies the flow pattern identification for the experimental data was based on the procedures suggested by Kim and Ghajar (2002) and visual observations deemed appropriate. All observations for the flow pattern judgments were made at two locations, just before the test section (about L/D = 93 in the calming section from the mixing well, see Fig. 3) and right after the test section. Leaving the liquid flow rate fixed, flow patterns were observed for various air flow rates. Flow pattern data were obtained with the pipe at horizontal position and at 2°, 5°, and 7° upward inclined positions. These experimental data were plotted and compared using their corresponding values of mass flow rates of air and water and the flow patterns. The digital images of each flow pattern at each inclination angle were also compared with each other in order to identify the inclination effect on the flow pattern.

Figure 5 shows photographs of the representative flow patterns that were observed in our experimental setup with the pipe in the horizontal position and no heating (isothermal runs). Figure 6 shows the flow map for our pipe in the horizontal position. The different flow patterns depicted on this figure illustrate the capability of our experimental setup in producing multitude of flow patterns. The shaded regions represent the boundaries of these flow patterns for the pipe in the horizontal position. Also shown on Fig. 6 with symbols is the distribution of the heat transfer data that were obtained systematically in our experimental setup with the pipe in the horizontal position. As can be seen from Fig. 6, we did not collect heat transfer data at low air and water flow rate combinations (water flow rates of less than about 5 kg/min and air flow rates of less than about 0.5 kg/min). At these low water and air flow rates and heating there is a strong possibility of either dry-out or local boiling which could damage the test section.

There are very few flow pattern data and flow pattern maps available in the literature for tubes with small angles of inclination. The influence of small upward inclination angles of 2°, 5°, and 7° on the observed flow patterns is shown in Fig. 7. This figure is a modified version of Fig. 6, which is based on the mass flow rate of each phase. As shown in Fig. 7, the shaded regions representing the transition boundaries of the flow patterns have shifted to the upper left direction for plug-

slug and slug-bubbly/slug transition due to the different inclination angles. The annular/bubbly/slug-annular transition boundaries appear to be insensitive to the slight inclination angles studied in this study. There are no drastic changes in the transition boundaries at the upward inclination angles of 2°, 5°, and 7° compared to the horizontal orientation. However, it should be mentioned that even though the flow pattern is named the same for both horizontal and inclined flows; it does not mean that the flow pattern in the inclined position has identical characteristics of the comparable flow pattern in the horizontal position. For example, it is observed that the slug flow patterns in the inclined positions of 5° and 7° have reverse flow between slugs due to the gravitational force, which can have a significant effect on the heat transfer.

Note that we have not taken flow pattern data below the liquid flow rate of about 5 kg/min for the inclined cases. Therefore, at this time we have no information on the influence of inclination angle on the flow pattern in this area. This is the subject of our near future investigations.

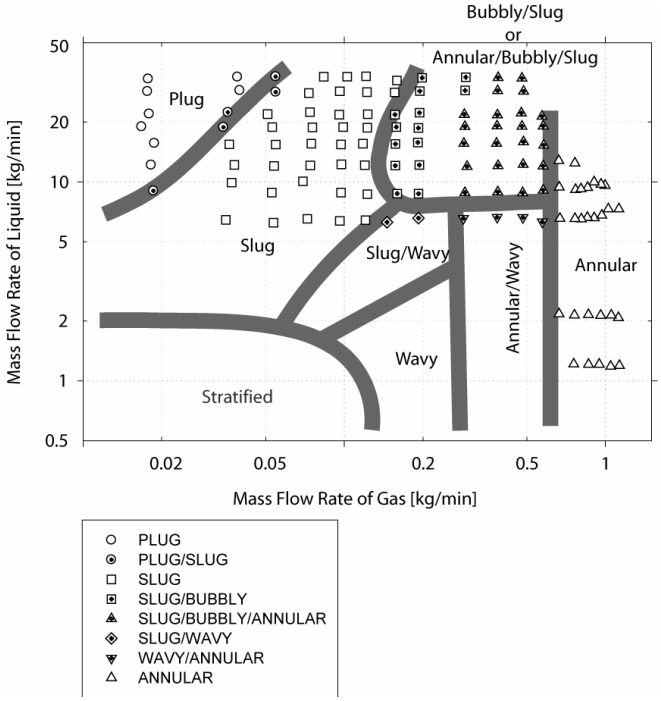

Figure 6. Flow map for horizontal flow.

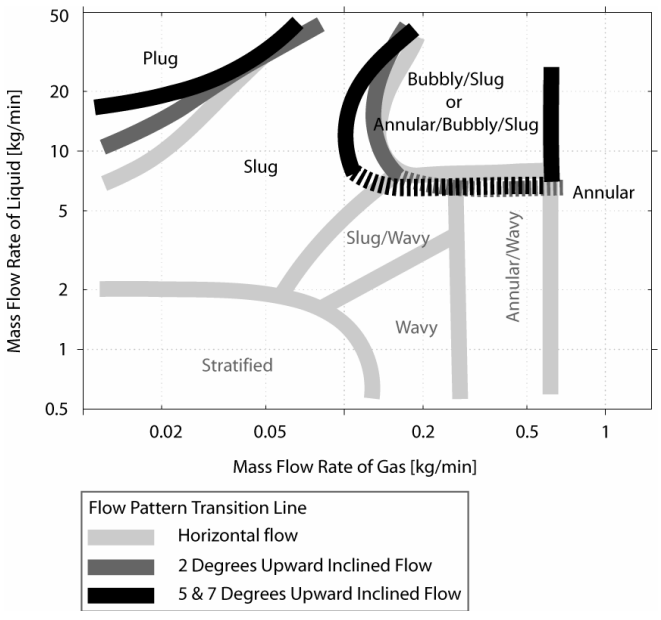

Figure 7. Change of flow pattern transition lines as pipe inclined upward from horizontal.

Systematic Investigation on Two-Phase Gas-Liquid Heat Transfer in Horizontal and Slightly Upward Inclined Pipe Flows

In this section we present an overview of the different trends that we have observed in the heat transfer behavior of the two-phase air-water flow in horizontal and inclined pipes for a variety of flow patterns. The two-phase heat transfer data were obtained by systematically varying the air or water flow rates and the pipe inclination angle.

Figure 8 provides an overview of the pronounced influence of the flow pattern, superficial liquid Reynolds number (water flow rate) and superficial gas Reynolds number (air flow rate) on the two-phase mean heat transfer coefficient in horizontal pipe flows. The results presented in Fig. 8(a) clearly show that two-phase mean heat transfer coefficients are strongly influenced by the liquid phase [liquid superficial Reynolds number (Re_{SL})]. As shown in Fig. 8(a), the heat transfer coefficient increases proportionally as Re_{SL} increases. In addition, for a fixed Re_{SL}, the two-phase mean heat transfer coefficients are also influenced by the gas superficial Reynolds number (Re_{SG}) and each flow pattern shows its own distinguished heat transfer trend as shown in Fig. 8(b). Typically, heat transfer increases at low Re_{SG} (the regime of plug flow), and then slightly decreases at the mid range of Re_{SG} (the regime of slug and slug-type transitional flows), and again increases at the high Re_{SG} (the regime of annular flow).

In order to conduct a more detailed comparison, the data matching the flow patterns between horizontal and inclined flows were selected and compared to see how much heat transfer increased in the inclined cases. Note that as the test section was inclined in the upward position, the flow patterns at certain cases were changed; for example, wavy-type transitional flow patterns in horizontal flow were changed to slug-type transitional flow patterns. A total of 68 horizontal flow data points were compared with their corresponding inclined flow data. The results are shown in Fig. 9. As shown in the figure, slug flow shows the biggest effect on two-phase heat transfer due to inclination. At the 5° upward inclined position, slug flow had an average increase of 45.3% against

horizontal flow. In contrast, annular flow, which is the flow mainly driven by inertia forces of gas phase, shows little effect on heat transfer due to inclination at 2° position.

Certain flow patterns, such as plug flow, slug/bubbly/annular flow, and annular flow, showed that the heat transfer rate increased as the test setup was inclined from 0° up to 7°. However, the other flow patterns, which are slug flow and slug/bubbly flow, had the maximum increase at the 5° inclination position, and then the effect of inclination was decreased at 7°. Most of all, the effect of inclination on the heat transfer of two-phase gas-liquid flow is significant in the slug and slug/bubbly flow patterns, which had an increase in the heat transfer which was much more than the average increase of 20% compared to the horizontal flow. The comparison results presented in Fig. 9 indicate that the slug and slug/bubbly flows show a much more pronounced enhancement in the two-phase heat transfer at all inclination angles in comparison to the other flow patterns shown (plug flow, slug/bubbly/annular flow, annular flow). The difference between the two groups of flow patterns has to do with the degree of mixing between each phase and the inertia force

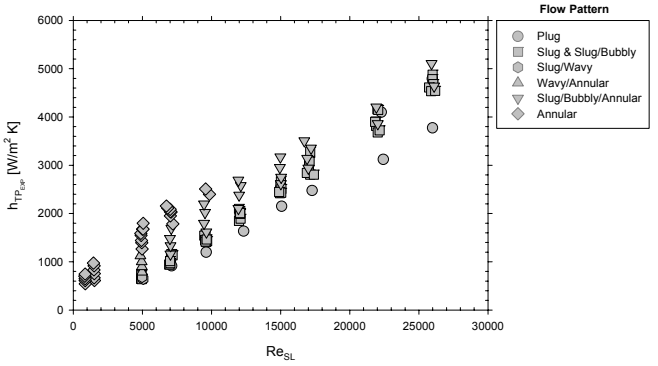

(a) h_{TP} vs. Re_{SL}

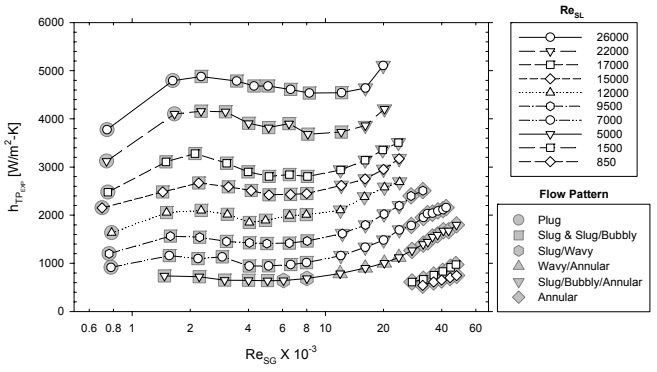

(b) h_{TP} vs. Re_{SG}

Figure 8. Variation of two-phase heat transfer coefficients with superficial liquid and gas reynolds numbers in a horizontal flow.

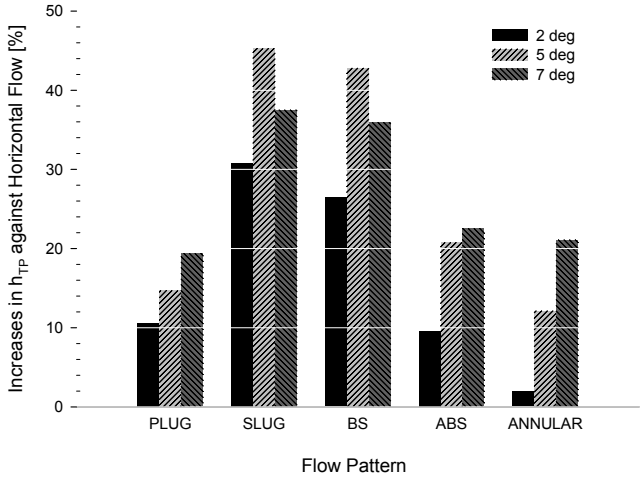

Figure 9. Increases of inclined flow h_{TP} against horizontal flow $h_{TP.}$

carried by each phase against the buoyancy force.

For a more detailed look at the effect of inclination on heat transfer in two-phase gas-liquid flow, the increase in h_{TP} versus Re_{SL} for each flow pattern is presented in Fig. 10. As shown in the figure, except for the case of annular flow, all other flow patterns indicated that the effect of the inclination at low Re_{SL} was significantly high and then decreased with increasing Re_{SL}. In the case of slug flow, the increase in the heat transfer was as much as 94% at Re_{SL} of around 5000 and at the 5° inclined position. However, it dropped to around 13% at Re_{SL} of around 25,000. This drop can be expressed as a drastic change in the effect of inclination on the heat transfer. The other flow patterns, except annular flow, show a similar trend as that of slug flow. These trends show that the increase of the inertia force in the fluid phases suppresses the effect of inclination.

The effect of inclination on heat transfer in non-boiling two-phase gas-liquid flow has been presented in many ways to better understand the mechanisms involved. As presented in this section, heat transfer in non-boiling two-phase gas-liquid flow is influenced by each of Re_{SL}, Re_{SG}, flow pattern, and inclination angle in a very complicated way. With increasing Re_{SL}, heat transfer proportionally increased regardless of the rest of the factors. By varying Re_{SG}, the distinguished trends of heat transfer by flow patterns were observed. Furthermore, significant changes were observed in the two-phase heat transfer of air-water flow with a slight upward inclination of the pipe from the horizontal position.

Heat Transfer Data Response to Flow Pattern and Inclination Factors

At the beginning of this paper, we developed a flow pattern factor, F_P, and an inclination factor, I, in order to handle

the various flow patterns and inclination angles in a gas-liquid pipe flow. Here, we have presented the response of our proposed flow pattern and inclination factors to our gas-liquid experimental data.

The effect of the flow pattern factor (F_P) on our data is shown in Figs. 11 and 12. In Fig. 11 we have plotted Eqs. (2) and (3) for the equilibrium wetted-perimeter relation $(1-\alpha)$ and the flow pattern factor (effective wetted-perimeter relation) against the Martinelli parameter (X). From this figure it is evident that the flow pattern factor (F_P) is clearly separated from the equilibrium wetted-perimeter $(1-\alpha)$ as the flow patterns change from plug to annular. This distinct separation between the flow patterns shown in Fig. 11 proves that the proposed flow pattern factor does an excellent job of distinguishing between the different flow patterns. Obviously this was not the case when the equilibrium wetted-perimeter relation $(1-\alpha)$ was used. In Fig. 12 the weighted all liquid heat transfer coefficients (h_L) are plotted as a function of the experimentally obtained two-phase flow heat transfer coefficients (h_{TP}). Here we see that by using the flow pattern factor as the weighting factor, the experimental heat transfer data all collapsed into one single curve and were very well represented [the shift in the data outside the ± 20% deviation band is because we did not introduce the rest of the correction factors given in Eq. (6)]. As shown in Fig. 12 with the use of equilibrium wetted-perimeter relation $(1-\alpha)$, the experimental data showed a very strong dependency on the flow pattern and were not well represented at all.

The effect of the inclination factor, I, on our data is shown in Fig. 13. In this figure we have plotted the inclination factor, see Eq. (5), against the superficial liquid Reynolds number (Re_{SL}). As shown in the figure, the effect of inclination on the data is clearly visible. The trends presented in Fig. 13 are very similar to those presented in Fig. 10 (h_{TP} vs. Re_{SL}) which showed the increases in the two-phase flow heat transfer as the test section was inclined.

The results presented in Figs. 11, 12, and 13 demonstrate that our proposed flow pattern and inclination factors are capable of handling the effects of different flow patterns and inclination angles. Based on these findings, we will next apply

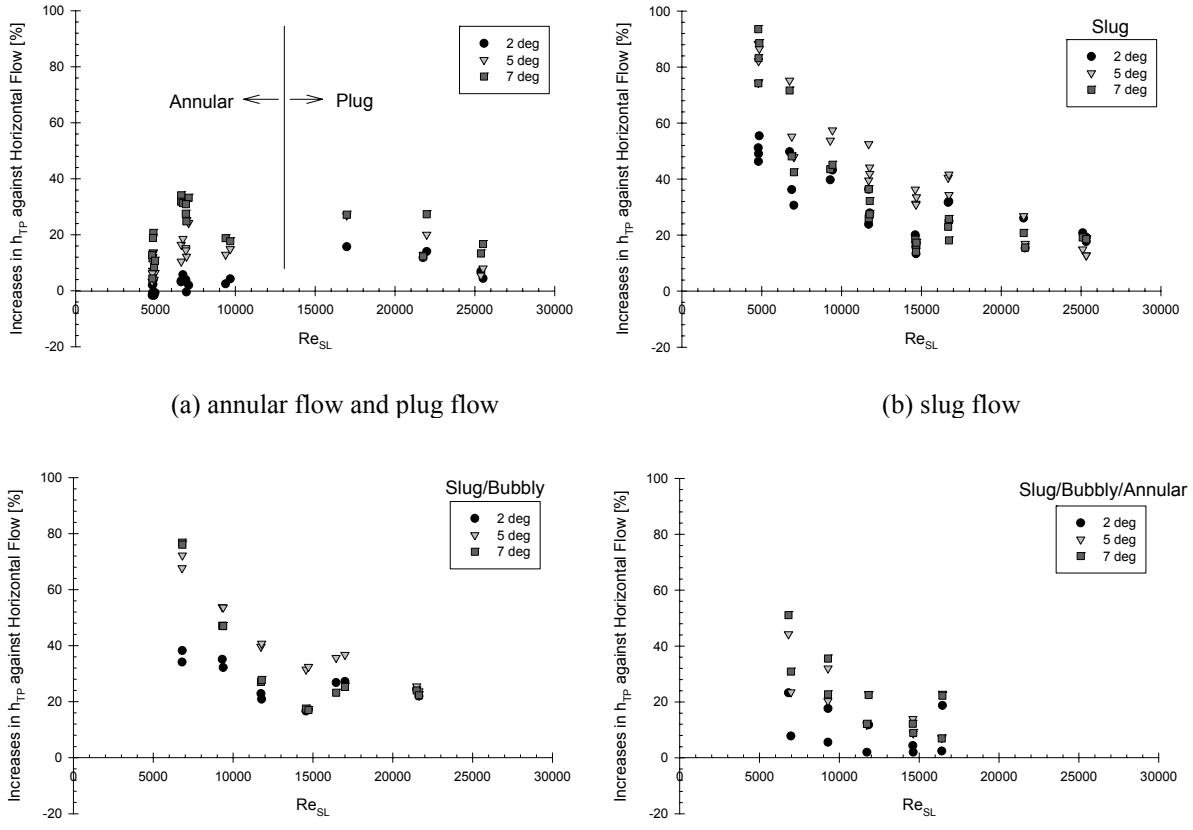

(a) annular flow and plug flow

(b) slug flow

(c) slug/bubbly flow

(b) slug/bubbly/annular flow

Figure 10 . Increases of inclined flow h_{TP} against horizontal flow h_{TP} by flow pattern.

our proposed heat transfer correlation, Eq. (6), to our experimental heat transfer data and determine the unknown coefficient and exponents of the correlation.

General Heat Transfer Correlation

In an earlier part of this paper we proposed a two-phase heat transfer correlation in the form given by Eq. (6). This correlation is designed to be capable of handling different flow patterns and inclination angles by means of introduction of a flow pattern factor (F_P) and an inclination factor (I) into the correlation.

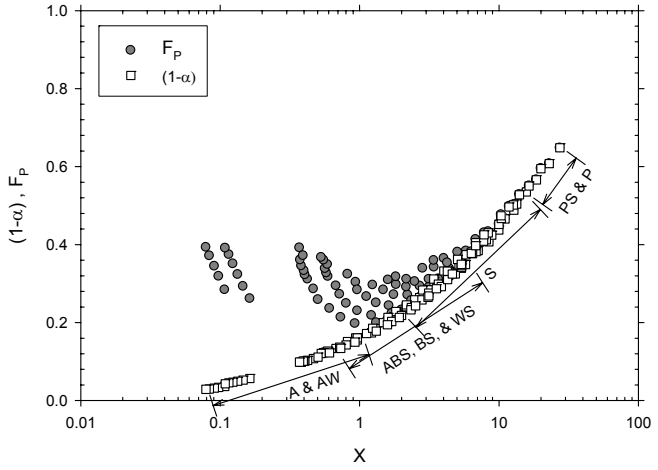

Figure 11. Equilibrium wetted-perimenter $(1-\alpha)$ and the flow pattern factor (F_P) for the horizontal flow experimental data.

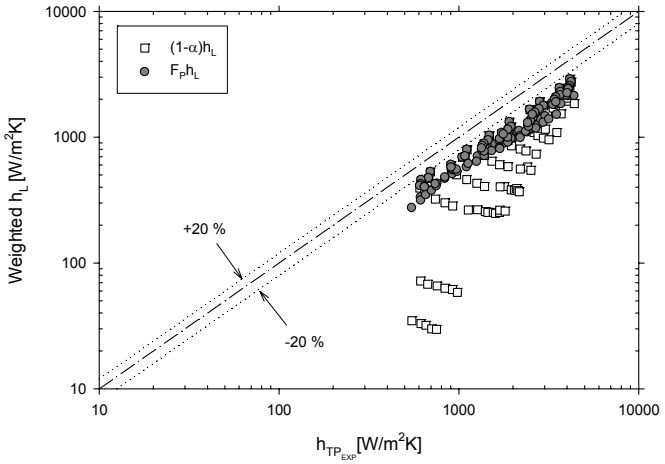

Figure 12. Weighted h_L by equilibrium wetted-perimeter term and the flow pattern factor for the horizontal flow experimental data.

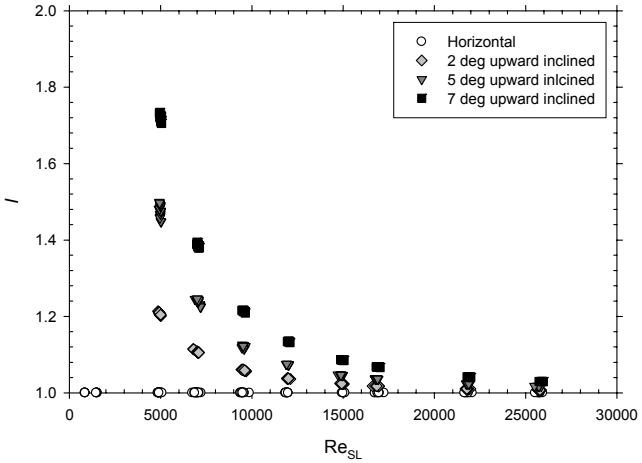

Figure 13. Inclination factor effect on the heat transfer experimental data.

To determine the values of the leading coefficient (C) and the exponents (m, n, p, q, r) in Eq. (6), the horizontal and inclined experimental data of Ghajar et al. (2004a,b,c) were used. A total of 408 data points with 114 points in the horizontal orientation, 100 points at 2° incline, 97 points at 5° incline, and 97 points in the 7° incline positions. Table 1 and Fig. 14 provide the details of the correlation and how well the proposed correlation predicted the experimental data. The correlation predicted the experimental data with an overall mean deviation of –4.22%, a standard deviation of 12.5%, and a deviation range of –30.7 to 37.0%. Ninety percent (90%) of all the experimental data were predicted within ± 20% deviation. Detailed results of the predictions by inclination angles and the range of the parameters used in the correlation are presented in Table 1.

These results provide additional validation on the robustness of our proposed two-phase heat transfer correlation. In addition, the modifications made to the general heat transfer correlation to account for the various flow patterns and the effect of inclination appears to be correct. We will continue our validation of the proposed general heat transfer correlation, Eq. (6), by comparing it with additional two-phase inclined heat transfer data for different flow patterns as the data becomes available from our laboratory and from the literature.

Table 1. Determined constants, results of predictions of the horizontal and inclined air-water flow experimental data, and the parameter range for Eq. (6).

Exp. Data (No. of Data)	Value of C and Exponents (m, n, p, q, r)						Mean Dev. [%]	Std. Dev. [%]	Dev. Range [%]	No. of Data within ± 20%	Range of Parameter					
	C	m	n	p	q	r					Re_{SL}	F_P	x	$\left(\frac{Pr_G}{Pr_L}\right)$	$\left(\frac{\mu_G}{\mu_L}\right)$	I
Total (408)	0.7	0.08	0.06	0.03	-0.14	0.65	-4.22	12.5	-30.7 to 37.0	367	835 to 25966	0.198 to 0.729	7.92×10^{-4} to 0.487	0.074 to 0.110	0.013 to 0.020	1.0 to 1.734
0 deg (114)							5.50	11.7	-18.3 to 37.0	106	835 to 25931	0.198 to 0.648	1.16×10^{-3} to 0.487	0.092 to 0.110	0.016 to 0.020	1.0
2 deg (100)							-5.02	9.1	-17.2 to 17.4	100	4858 to 25845	0.211 to 0.716	8.90×10^{-4} to 0.123	0.081 to 0.087	0.015 to 0.016	1.007 to 1.214
5 deg (97)							-9.51	11.1	-24.2 to 23.6	83	4907 to 25854	0.214 to 0.729	7.92×10^{-4} to 0.117	0.073 to 0.081	0.013 to 0.015	1.018 to 1.499
7 deg (97)							-9.53	11.3	-30.7 to 25.6	78	4928 to 25966	0.211 to 0.697	9.46×10^{-4} to 0.124	0.083 to 0.089	0.016 to 0.015	1.029 to 1.734

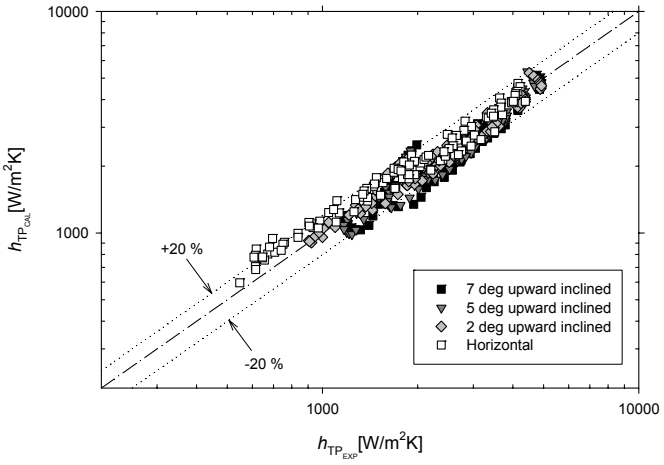

Figure 14. Comparison of the predictions of the recommended heat transfer correlation with the heat tansfer data.

CONCLUSION

The purpose of this study was to further develop the knowledge and understanding of heat transfer in non-boiling two-phase, two-component flow. For this purpose air-water flow heat transfer experiments were conducted in a circular pipe in the horizontal and slightly upward inclined positions at 2°, 5°, and 7° under uniform wall heat flux boundary condition.

In the case of heat transfer in horizontal flow, the heat transfer rate proportionally increased as Re_{SL} increased. However, in more detail, it is observed that heat transfer shows distinguished trends depending on the flow pattern and Re_{SG}. The effect of inclination was significant on heat transfer in two-phase flow and had different characteristics depending on the flow pattern. The data showed that heat transfer coefficient increased up to around 90% for slug flow at 5° inclined position and at low Re_{SL} range. However, the effect of inclination was quickly diminished as Re_{SL} increased. In contrast, annular flow showed little effect on heat transfer due to inclination at lower inclination angle and Re_{SL}. However, annular flow showed that the heat transfer rate increased with increasing inclination angle and Re_{SL} compared to the horizontal flow.

This study also led to the development of a general overall heat transfer coefficient correlation for gas-liquid two-phase flow regardless of flow pattern and pipe orientation. In order to properly account for the effect of different flow patterns and

inclination angles on the heat transfer in two-phase flow, a flow pattern factor (F_P) and an inclination factor (I) were designed and introduced into the heat transfer correlation. The data collected in this study for different flow patters and inclination angles were successfully predicted by the proposed general heat transfer correlation.

ACKNOWLEDGEMENTS

The authors gratefully acknowledge the financial support provided by the Oklahoma State University (OSU) Foundation and Micro Motion, Omega, Dell Computers, and National Instruments for their generous contributions and consideration to the modernization of the laboratory.

REFERENCES

Chisholm, D. (1973), Two-Phase Flow in Pipelines and Heat Exchangers, George Godwin, London and New York in association with the Institution of Chemical Engineers, New York.

Durant, W. B. (2003), "Heat Transfer Measurement of Annular Two-Phase Flow in Horizontal and a Slightly Upward Inclined Tube," M.S. Thesis, Oklahoma State University, Stillwater, OK.

Ghajar, A. J. (2004), "Non-Boiling Heat Transfer in Gas-Liquid Flow in Pipes – a Tutorial," *ENCIT2004: Proc. of the 10th Brazilian Congress of Thermal Sciences and Engineering*, Nov. 29-Dec. 3, Rio de Janeiro, Brazil.

Ghajar, A. J. and Zurigat, Y. H. (1991), "Microcomputer-Assisted Heat Transfer Measurement /Analysis in aCircular Tube," Int. J.Applied Engineering Education, vol. 7, no. 2, pp. 125–134.

Ghajar, A. J., Kim, J., Durant, W. B., and Trimble, S.A. (2004a), "An Experimental Study of Heat Transfer in Annular Two-Phase Flow in A Horizontal and Slightly Upward Inclined Tube," *HEFAT2004: Proc. 3rd International Conference on Heat Transfer, Fluid Mechanics and Thermodynamics*, June 21-24, Cape Town, South Africa, Paper No. GA1.

Ghajar, A. J., Kim, J., Malhotra, K., and Trimble, S.A. (2004b), "Systematic Heat Transfer Measurements for Air-Water Two-Phase Flow in a Horizontal and Slightly Upward Inclined Pipe," *ENCIT2004: Proc. of the 10th Brazilian Congress of Thermal Sciences and Engineering*, Nov. 29-Dec. 3, Rio de Janeiro, Brazil, Paper No. CIT04-0471.

Ghajar, A. J., Malhotra, K., Kim, J., and Trimble, S. A. (2004c), "Heat Transfer Measurements and Correlations for Air-Water Two-Phase Slug Flow in a Horizontal Pipe," *HT-FED2004: Proc. of 2004 ASME Heat Transfer/Fluids Engineering Summer Conference*, July 11-15, Charlotte, North Carolina, Paper No. HT-FED2004-56614.

Hetsroni, G., Hu, B. G., Yi, B. G., Mosyak, A., Yarin, L. P., and Ziskind, G. (1998), "Heat Transfer in Intermittent Air-Water Flow–Part II: Upward Inclined Tube," Int. J. Multiphase Flow, vol. 24, no. 2, pp. 188–212.

Kim, D. and Ghajar, A. J. (2002), "Heat Transfer Measurements and Correlations for Air-Water Flow of Different Flow Patterns in a Horizontal Pipe," Experimental Thermal and Fluid Science, vol. 25, pp. 659–676.

Kim D., Ghajar A. J., and Dougherty R. L. (2000), "Robust Heat Transfer Correlation for Turbulent Gas-Liquid Flow in Vertical Pipes," J. Thermophysics and Heat Transfer, vol. 14, no. 4, pp. 574–578.

Kim, D., Ghajar, A. J., Dougherty, R. L., and Ryali, V. K. (1999), "Comparison of 20 Two-Phase Heat Transfer Correlations with Seven Sets of Experimental Data, Including Flow Pattern and Tube Inclination Effects," Heat Transfer Engineering, vol. 20, no. 1, pp. 15–40.

Kline, S. J. and McClintock, F. A. (1953), "Describing Uncertainties in Single-Sample Experiments," *Mech. Engr.*, vol. 1, pp. 3-8.

Sieder, E.N. and Tate, G.E. (1936), "Heat Transfer and Pressure Drop of Liquids in Tubes," Industrial & Engineering Chemistry, vol. 28, no. 12, pp. 1429–1435.

Trimble, S. A., Kim, J., and Ghajar, A. J. (2002), "Experimental Heat Transfer Comparison in Air-Water Slug Flow in Slightly Upward Inclined Tube," In Proc. 12th International Heat Transfer Conference, Heat Transfer 2002, pp. 569–574, Elsevier.

